Applied Catalysis A: General 398 (2011) 59–65

Contents lists available at ScienceDirect

Applied Catalysis A: General

journal homepage: www.elsevier.com/locate/apcata

Efficiency of ethanol conversion induced by controlled modification of pore structure and acidic properties of alumina catalysts

Leandro Martins[a,*], Dilson Cardoso[b], Peter Hammer[a], Teresita Garetto[c], Sandra H. Pulcinelli[a], Celso V. Santilli[a]

[a] Instituto de Química, UNESP – Univ Estadual Paulista, Prof. Francisco Degni SN, 14800-900 Araraquara, SP, Brazil
[b] Departamento de Engenharia Química, UFSCar – Univ Federal de São Carlos, Rod. Washington Luis Km 235, 13565-905 São Carlos, SP, Brazil
[c] Instituto de Investigaciones en Catálisis y Petroquímica, (INCAPE) UNL-CONICET RA-3000 Santa Fe, Argentina

ARTICLE INFO

Article history:
Received 19 January 2011
Received in revised form 2 March 2011
Accepted 6 March 2011
Available online 11 March 2011

Keywords:
Macroporous materials
Mesoporous materials
Alumina
Emulsion
Ethanol dehydration

ABSTRACT

Bimodal porous alumina catalysts with both continuous macropores and mesopores were prepared using a dual soft template method. The addition of decahydronaphthalene as emulsifier agent successfully contributed to the formation of macropores. The effectiveness of macropore insertion was evaluated in the model reaction of ethanol dehydration at 300 °C. Judging from the results obtained by acidity measurements using temperature programmed desorption of ammonia and the performance of these catalysts in the ethanol dehydration, the introduction of macropores in the catalyst structure enhanced the ethanol conversion.

1. Introduction

Continuous reactors are preferred in most industrial processes because the reaction proceeds with the highest yield of product and require the lowest amount of operation costs [1]. In these continuous catalytic processes granulated heterogeneous catalysts are needed, since the drawbacks of fine powders, such as high hydraulic head loss, is avoided.

In the fabrication of these pellets the powder catalysts are pressed into different forms such as spheres or rods. In this pelletization process most of the large macropores (typically > 0.5 μm) that are formed in the interparticle region are removed while both the mesopores and micropores prevail in the pellets [2]. The diffusion rate of reactants and products in these small pores is lowered and this affects the overall kinetics of reaction especially for those taking place in highly active catalysts [3]. In this context, the development of porous ceramics with controlled intraparticle macroporosity has attracted considerable attention as potential catalyst supports. This is in particular the case of bimodal systems containing macropores which are not formed in the void space between powder particles. Furthermore, hierarchically fabricated porous ceramics enclosing macropores and mesopores exhibit extremely high porosities [4,5], with a significant degree of interconnectivity that results in low reactor pressure-drop and high molecular diffusion rate [6].

Alumina is one of the most widely used materials in heterogeneous catalysis due to several attractive features [7]. Therefore, any improvement in reactions yield is extremely profitable, considering the quantity and variety of chemicals produced through alumina supported catalysts. Recently, we have reported a simple and useful procedure for the preparation of hierarchically structured porous aluminas [4]. This procedure uses a combination of the sol–gel route and a dual soft template technique involving dispersed oil droplets (emulsified "oil in water" system) and block copolymer micelles. By using this strategy, a series of hierarchical alumina macro-mesoporous structures presenting controlled amount of macroporosity were easily obtained.

This paper reports the catalytic results obtained for ethanol dehydration on several alumina supports to evaluate the role of mesopores and macropores on the overall reaction activity. Ethanol dehydration was chosen as a probe reaction to develop a basic comprehension of the effects of porosity on catalysis of aluminas prepared by a dual soft templating method. Apart from the characteristic of probe reaction ethanol conversion represents an important environmental issue, because nowadays the search for alternative sources of chemicals is an authentic challenge [8].

* Corresponding author. Tel.: +55 16 3301 9705; fax: +55 16 3301 9692.
E-mail address: leandro@iq.unesp.br (L. Martins).

0926-860X/$ – see front matter © 2011 Elsevier B.V. All rights reserved.
doi:10.1016/j.apcata.2011.03.014

2. Experimental

2.1. Preparation of the porous aluminas

The porous aluminas were prepared according to a procedure described in [4]. The used reagents were Pluronic P123 (the tradename for a triblock copolymer, whose nominal formula is $HO(CH_2CH_2O)_{20}(CH_2CH(CH_3)O)_{70}(CH_2CH_2O)_{20}H$, used as surfactant and mesopore template), decahydronaphthalene (DHN, used as emulsion and macropore template), aluminum isopropoxide ($Al(i\text{-}OPr)_3$), n-pentanol (cosurfactant) and nitric acid. A homogeneous and clear sol was obtained with the following molar composition: 0.015Plunonic P123:1Al(i-$OPr)_3$:0.1n-pentanol:1.5HNO_3:35H_2O.

After the sol preparation, emulsification was performed by adding DHN under magnetic stirring for 5 min. Gelation was induced by adding a controlled amount of NH_4OH solution (29 wt.%) drop by drop into this medium under mechanical stirring up to pH equal to 4.0. The quantity of DHN used was varied according to: 0, 50, 60 and 70 wt.%, and the samples were referred as Al-1, Al-2, Al-3 and Al-4, respectively. A reference sample denoted Al-ref was prepared following the same procedure however without the addition of emulsion and surfactant.

In a previous work [4] aluminas containing different DHN quantities (0, 15, 30, 50, 60 and 70 wt.%) were prepared and studied in detail regarding the preparation method. The results showed that there was almost no difference in properties between aluminas prepared with DHN content of 15 and 30 wt.%, *i.e.* only a slight change in porosity was observed in comparison to the alumina reference. On the other hand, samples prepared with DHN varying between 50 and 70 wt.% were those with largest differences in porosity. Therefore, this work was focused only on samples in this concentration range.

The calcination was carried out in a conventional muffle oven by increasing the temperature (5 °C/min) from room temperature to 190 °C, then heating (1 °C/min) to 600 °C and kept at this temperature for 2 h.

Despite the use of significant amounts of decahydronaftalene as macropore template in preparation of samples (up to 70 wt.%), this compound is completely volatilized at 190 °C during calcination of aluminas. The thermal behavior of the as-synthesized samples was investigated by thermo-gravimetric analysis, performed from room temperature up to 800 °C under air flow. The results published in Ref. [4] have shown a significant weight loss only up to 500 °C. All samples were calcined at 600 °C in air environment and their visual aspect after that was of a white powder, suggesting the absence of carbon residue.

2.2. Catalytic reaction – ethanol dehydration

The alcohol conversion was monitored in a plug flow reactor fitted with a thermocouple extending to the center of the catalyst bed. Reaction data were collected under atmospheric pressure using 50 mg of catalyst. Liquid ethanol (99.8% Merck) was pumped into the heated reactor (1 mL/h) using a syringe pump where it was mixed with 25 mL/min of nitrogen gas, delivered by a mass flow controller, to adjust the reactor feed composition. All the connection lines were heated to 150 °C to prevent condensation. The composition of the reactor effluent stream was analyzed using a gas chromatograph equipped with a flame ionization detector (FID). The chromatograph was connected online to the reactor outlet. A DB-1 capillary column was used in the analysis of the product stream. At a temperature of 50 °C in GC analysis, ethene, acetaldehyde, ethanol and diethyl ether peaks were observed at 5, 5.9, 6.1 and 7.1 min, respectively. The calibration was carried out using a mixture of reactant and products of known composition. Catalysts were dried at 200 °C in situ under nitrogen stream before the experiments. Data were collected every 7 min while the reaction temperature was increased from 150 to 300 °C. Each data point corresponds to an average of results obtained for at least four successive measurements.

2.3. Characterization

The pore size distribution was determined by mercury intrusion porosimetry using the AUTOPORE III equipment (Micromeritics). All samples were degassed before analysis at a vacuum pressure below 5×10^{-5} Pa. The pore diameter was calculated from the Washburn equation [9], using standard surface tension and contact angle values of 0.489 N/m and 135°, respectively. The size of alumina macropores was also determined from scanning electron micrographs, recorded using a Philips XL 30 equipment. For this purpose the samples were fixed on aluminum sample holder and sputtered with gold.

The powder skeletal density (ρ_s) was determined with an AccuPyc 1330 equipment (Micromeritics) utilizing helium gas. Samples were purged 10 times before measurements. Ten replicates were automatically made for each sample, and the mean value was used. The bulk density (ρ_b) was measured with a GeoPyc 1360 equipment (Micromeritics), using a free-flowing dry powder (DryFlo) as the displaced medium. The porosity ($P\%$) was calculated from the density values by using the relation $P\% = (1 - \rho_b/\rho_s) \times 100$.

Nitrogen adsorption–desorption isotherms were recorded at liquid nitrogen temperature and relative pressure interval between 0.001 and 0.998 on the equipment supplied by Micromeritics (ASAP 2010). Samples were evacuated prior to measurements at 200 °C for 12 h under vacuum of 1×10^{-5} Pa. Surface areas were calculated following the BET equation up to $P/P_o = 0.3$.

The crystalline phases present in calcined samples were analyzed by X-ray diffraction (XRD) using a Siemens D5000 diffractometer and Cu Kα radiation selected by a curved graphite monochromator. The phase identification was done using the program X'Pert High Score and the crystallographic pattern file [04–0875] for γ-Al_2O_3 and [70–2038] for γ-$Al(OH)_3$ (gibbsite).

Acid sites in calcined aluminas were determined by temperature programmed desorption of ammonia (TPD-NH_3) in a Micromeritics ChemiSorb 2705. Samples were treated in helium at 300 °C for 30 min and then exposed to a 1% of ammonia (v/v in helium) stream at 100 °C until surface saturation. The ammonia excess was removed with a helium flow at 100 °C until a constant baseline signal was obtained. The TPD-NH_3 analyses were started by heating the sample 10 °C/min from 25 to 800 °C under helium flow (60 mL/min). The amount of desorbed ammonia per gram of sample was estimated by the thermal conductivity detector response.

The XPS measurements were carried out using a commercial spectrometer (UNI-SPECS UHV). The Mg Kα line was used ($h\nu$ = 1253.6 eV) and the analyzer pass energy was set to 10 eV. The inelastic background of the C 1s, O 1s and Al 2p core-level spectra was subtracted using Shirley's method. The binding energies of the spectra were corrected using the hydrocarbon component of adventitious carbon fixed at 285.0 eV. The composition of the surface layer was determined from the ratios of the relative peak areas corrected by sensitivity factors for the corresponding elements. The deconvoluted spectral components were obtained using multiple Voigt profiles (70% Gaussian and 30% Lorentzian) without placing constraints. The width at half maximum (FWHM) varied between 1.5 and 2.2 eV, and the accuracy of the peak positions was ±0.1 eV. The small component at high binding energy tail of the O 1s spectra, attributed to physisorbed carboxyl groups, was subtracted from all envelope spectra.

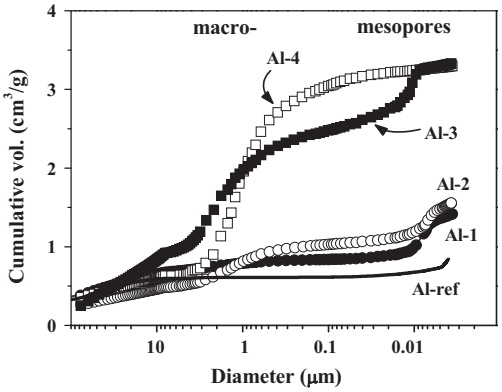

Fig. 1. Effect of DHN amount on the cumulative pore volume determined by Hg-porosimetry.

3. Results and discussion

3.1. Porous aluminas characterization

The effects of DHN amount on the cumulative pore size distribution of the calcined aluminas are presented in Fig. 1. A bimodal size distribution, named as macro- (close to 1 μm) and meso- (in the range of 8–9 nm) pores families can be observed. Sample Al-1 was prepared without DHN addition, *i.e.* containing only the surfactant, for comparison with samples Al-2 to Al-4. The pore size distribution in the mesopore region is present in all samples from Al-1 to Al-3, and we attribute this pore family to the micelle templating process. Sample Al-4 presents only the macropore family, despite the addition of the surfactant in the gel synthesis. A possible explanation for the absence of the mesopore family in this sample is the migration of surfactants from the micelles to the oil/water interface. This is comprehensible since the amount of DHN is quite high, 70 wt.%. Furthermore, a considerable increase of the specific macropore volume can be observed when increasing the DHN quantity from 50 to 70%, in samples Al-2 to Al-4, respectively.

Representative scanning electron microscopy (SEM) images of the alumina samples (Fig. 2) provide additional evidence for the presence of macropores in the samples prepared with DHN. The alumina morphology is composed of three-dimensionally interconnected pores with circular cross section and diameter varying from 0.1 to 2 μm. Despite the variation of the macropores diameter they were found to show a relatively narrow size distribution centered on 1 μm. It is important to note that the alumina pore structure presents a good thermal stability, thus after calcination in air at 600 °C the porous structure remained stable and no significant amount of cracking was observed.

These experimental results demonstrate that aluminas with pores at two distinct length scales can be produced using adequate synthesis conditions. Additionally, the findings obtained for the set of conditions used in this study suggest that the formation of these two different characteristic pore morphologies can be decoupled since they can be individually adjusted by controlling the surfactant or the oil concentration.

Table 1 displays some characteristics of the porous aluminas such as macro/mesopore volume, porosity and BET surface area, including the reference sample, Al-ref that was prepared without addition of surfactant and DHN to evidence the additive contribution of both templates in generating the observed porosity. It can be observed that the addition of DHN significantly increases the macropore volume up to 2.41 cm^3/g. This is reflected by the values of the bulk density and sample porosity, the last increasing from 71 to 94%. Although, no systematic change was observed for the BET surface area, a considerably higher value was determined for the Al-3 as compared to the reference.

Fig. 3a shows that as-synthesized samples present a not very well defined X-ray diffraction pattern. XRD results shown in Fig. 3b reveal the formation of a typical γ-Al_2O_3 structure after calcination [10], which is independent of the content of DHN and surfactant templates (Table 1). Additionally, Fig. 3a shows peaks related to the presence NH_4NO_3, resulting from the use of NH_4OH and HNO_3 in the synthesis, the latter is easily washed away. SEM observation of alumina samples before and after the calcination revealed that this phase transformation is topotactic, thus both the particles and the pores morphology remain unchanged.

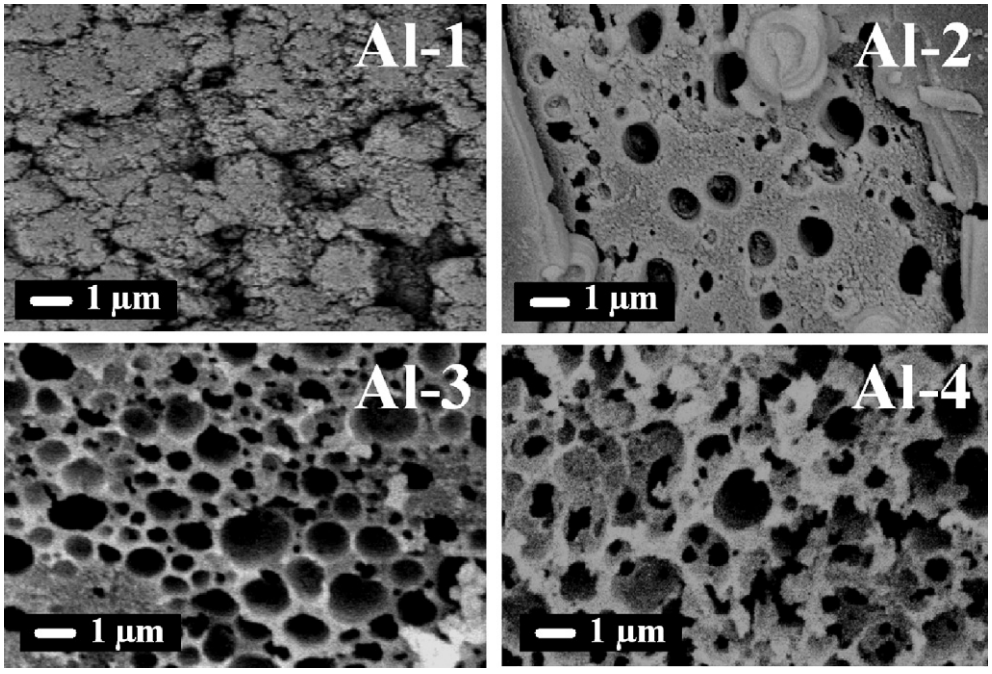

Fig. 2. Scanning electron micrographies of Al-1 to Al-4 aluminas samples.

Table 1
Pore volume, bulk density, porosity and BET surface area of the alumina samples prepared with different DHN content.

Sample	$Vol._{DHN}/Vol._{Sol}$[a]	DHN (wt.%)	V_{meso} (cm^3/g)	V_{macro} (cm^3/g)	Bulk density (g/cm^3)	Porosity (%)	BET_{Area} (m^2/g)
Al-ref	0	0	0.16	0.02	0.85	71	362
Al-1	0	0	0.50	0.15	0.58	82	352
Al-2	1.1	50	0.45	0.54	0.37	89	293
Al-3	1.7	60	0.52	1.63	0.32	92	473
Al-4	2.6	70	0.08	2.41	0.27	94	417

[a] Volume of added DHN in relation to the volume of the alumina sol.

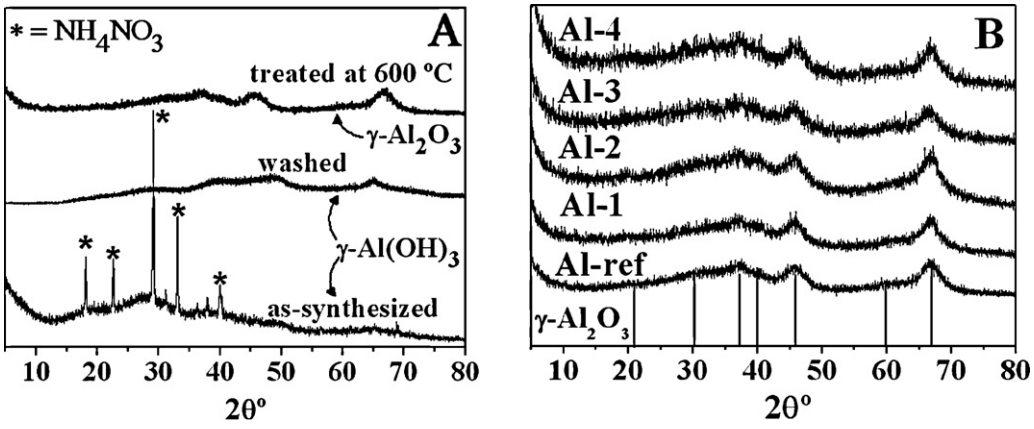

Fig. 3. XRD patterns of alumina samples prepared (a) without the addition of surfactant and DHN and (b) with different DHN quantity and calcined at 600 °C.

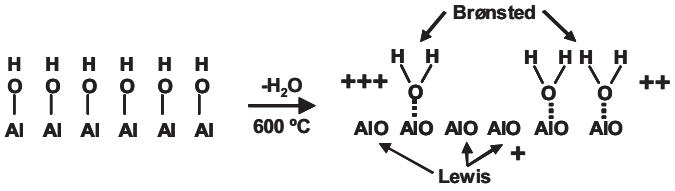

Scheme 1. Representation of the nature of acid sites on alumina surface (acid strength +++ > ++ > +).

As shown in Scheme 1, not only the structure of aluminas but also the surface of calcined samples can change completely upon firing. The transition alumina γ-Al_2O_3 is formed from oxyhydroxides and hydroxides under various dehydration and dehydroxylation conditions, in which these two descriptions represent the loss of water by desorption of physisorbed water or by condensation of hydroxyl groups, respectively. Scheme 1 represents the dehydroxylation condition, in which two adjacent surface hydroxyls condense to form water molecules on the surface during the formation of γ-Al_2O_3 at 600 °C. This dehydroxylation can be represented as $\sim OH + \sim OH \rightarrow \sim O\sim + \square + H_2O$, where $\square$ represents an oxygen vacancy, an electron-deficient metal atom, upon formation of 4- or 5-coordinated AlO_x sites from 6-coordinated ones [11].

The spectral analysis of the XPS data of calcined samples, which was focused on O 1s core-level spectra, provided additional information about the hydroxyl concentration on the surface of the alumina samples. The deconvolution of the O 1s spectra into two components depicted in Fig. 4 and Table 2, allowed to obtain information regarding the relative amount of oxygen bonded in the form of aluminum oxide (530.5 eV) or superficial hydroxyl groups (531.7 eV). The XPS signal related to the hydroxyl groups decreases continuously with the addition of DHN. This result highlights a general tendency, also observed in NH_3-TPD measurements, that the addition of DHN interferes in the quantity of hydroxyl groups available on the surface (Fig. 5). Probably the interaction of the surfactant with aluminum species occurs via oxygen atoms of the surfactant with the hydrogen atoms of the oxyhydroxides, inducing the formation of hydroxyls at the interface. As already verified, as the

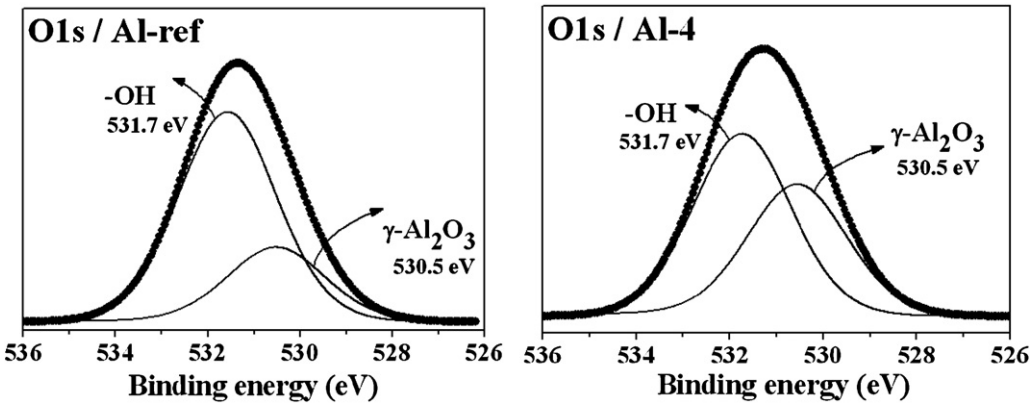

Fig. 4. O 1s spectra of the Al-ref and Al-4 alumina samples.

Table 2
XPS signals distribution and amount of acid sites obtained from TPD-NH_3 profiles from calcined samples.

Sample	XPS signals (%)		TPD acid sites distribution			Total acid sites normalized by	
	Hydroxyls	Al_2O_3	Weak (%)	Moderate (%)	Strong (%)	Mass (mmol NH_3/g)	Area (μmol NH_3/m^2)
Al-ref	73.9	26.1	30.0	34.7	35.3	7.9	21.8
Al-1	64.6	35.4	75.1	24.9	0	7.2	20.4
Al-2	61.3	38.7	78.6	21.4	0	6.7	22.8
Al-3	59.5	40.5	100	0	0	8.4	17.8
Al-4	57.5	42.5	100	0	0	8.3	20.0

quantity of DHN increases up to 70 wt.%, the surfactants present in the sol migrate to the DHN/water interface diminishing their amount in the continuous aqueous phase and interfering strongly on the presence of surface hydroxyls.

Considering that γ-Al_2O_3 has special importance in catalytic applications, the samples were evaluated on their acid properties using temperature programmed desorption of NH_3 (NH_3-TPD). An ammonia molecule can be retained on the surface of alumina in two different modes: (1) transfer of a proton from surface hydroxyl to the adsorbate; this occurs with the surface acting as a Brønsted acid, corresponding to the strongest mode of interaction and (2) coordination to an electron-deficient aluminum atom; taking place with the solid acting as a Lewis acid, created by dehydroxylating of the surface. If NH_3 adsorption takes place with a Brønsted acid site, the interaction can involve neighboring hydroxyl groups with different acidic strengths, denoted according to Scheme 1 as ++ or +++. This acid strength distribution results in a broad NH_3 desorption profile.

Fig. 5 shows that all aluminas have a large amount of weak acid sites, probably Lewis sites (temperature of desorption between 100 and 230 °C). However only samples without or with lower DHN quantity owns strong acid sites able to retain NH_3 from 250 to 300 °C or even higher, probably of Brønsted nature. The quantity of desorbed NH_3 at high temperatures is quite low, especially in samples Al-3 and Al-4, indicating that the strong acid sites present in these alumina surfaces are irrelevant. Evidently, this is a consequence of an inductive effect of DHN on oxyhydroxides at alumina surface during the synthesis. The broad desorption peaks also reveals that the alumina samples possess a heterogeneous distribution of both type of acid sites. This distribution was already observed by pyridine adsorption followed by Fourier transform infrared spectroscopy [12].

Table 2 reports the relative amount of acid sites of type 1, 2 or 3 (weak, moderate or strong) able to adsorb NH_3. The total amount of acid sites determined either per mass of catalyst or per surface area is practically equal for all alumina samples, while the strong acid sites decrease with the addition of DHN. The differences in the concentration of these acid sites will strongly affect the catalytic performance of these aluminas, as we will discuss further on.

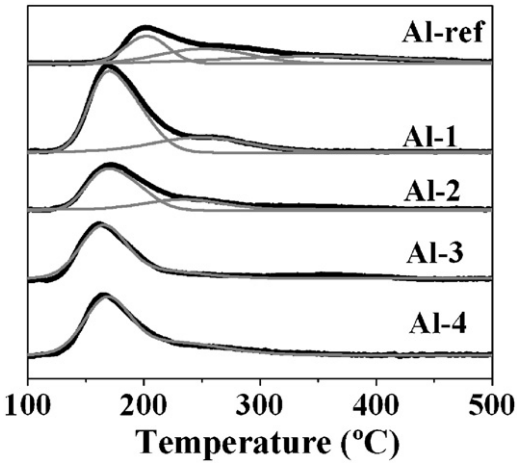

Fig. 5. NH_3-TPD curves (black) and deconvolution profiles (grey) of the aluminas prepared with different amounts of DHN.

3.2. Catalytic activity on ethanol dehydration reaction

Ethanol dehydration is commonly used to characterize the acid strength of solid catalysts [13]. Ethanol conversion can be acid or base catalyzed, therefore the selectivity to a desired product can be easily related to the character of the surface. Therefore this reaction was selected to examine catalytic performance of the alumina samples. A simplified ethanol dehydration reaction is depicted in Scheme 2, showing that there are two pathways for product formation based on acid (k_a) or basic sites (k_b) [13]. The porous aluminas studied in this work led mainly to the formation of ethene and diethyl ether with minor amount of acetaldehyde (<0.5% selectivity), thus demonstrating the prevailing acidic character of the catalysts. At low temperature diethyl ether is produced, while at high temperature ethene is predominantly produced, as a consequence of intramolecular dehydration [13]. Besides those products sketched in Scheme 2, no other was detected in any of the experimental conditions used here.

Fig. 6 shows the ethanol dehydration results obtained at 300 °C using the porous alumina catalysts. The samples are ordered according to the increasing porosity and decreasing acidity. The result is quite surprising, the conversion passes through a minimum (Fig. 6a and b). For the sample Al-ref, which presented the highest concentration of hydroxyl groups on the surface, the most efficient conversion was detected. This result is related to the higher ability of Brønsted acid sites to activate ethanol molecule. Furthermore Fig. 6 shows that for the Al-4, with the highest porosity, the ethanol conversion is comparable to Al-ref. In spite of Al-4 presents the lowest acidity, this behavior can be related to easier reactants and products diffusion in the catalyst pores. Although ethanol is a small molecule compared to pore dimensions of the studied alumina, its conversion seems to be to some extend a pore diffusion controlled reaction, that is, the activity appears to be related to catalyst porosity. Therefore, this behavior highlights both the contribution of catalyst acidity and porosity on the ethanol conversion. The region of minimum observed for sample Al-2 represents the worst combination of catalyst acidity and porosity.

Indeed, ethanol dehydration proceeds initially via the adsorption of the ethanol molecule and the O–H bond rupture on acid sites giving rise to a surface ethoxy group. More strongly

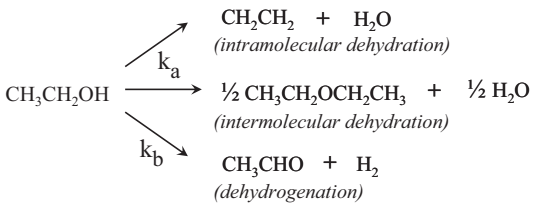

Scheme 2. Reaction scheme of ethanol conversion on acid (k_a) and basic (k_b) catalysts.

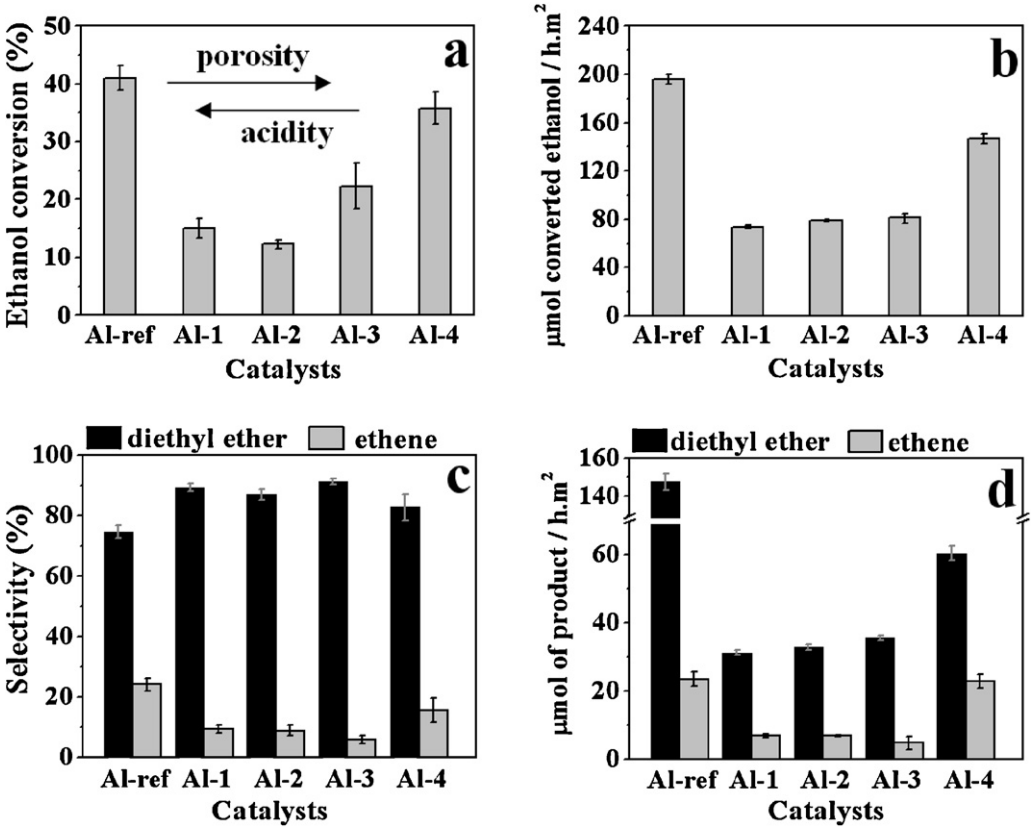

Fig. 6. Catalytic results of ethanol dehydration of alumina samples at 300 °C: (a) ethanol conversion, (b) ethanol molar consumption normalized by aluminas surface area, (c) product selectivity and (d) products molar formation normalized by aluminas surface area.

adsorbed ethanol favors O–H bond rupture facilitating the nucleophilic attack and consequently giving rise to higher conversion [13]. For this reason the most acidic sample Al-ref was the most active. However, in the case of Al-4 sample that showed a relative weak acidity, facilitated diffusion through its porous structure might have mainly contributed to the observed ethanol conversion [14,15].

The formation of diethyl ether (Fig. 6c and d) is a reaction that involves two adjacent alcohol molecules adsorbed on two neighboring sites [13,16]. This is the reason why diethyl ether selectivity is favorable at low conversion levels, thus decreasing with increasing conversion. On the other hand, ethene formation occurs via intramolecular dehydration and is predominant at high conversions as shown in Fig. 7. At low temperatures (Fig. 7a), not only the catalyst activity is poor, but also the selectivity of ethylene is low due to a large number of ethanol converted to diethyl ether. The change in the relative abundance of Lewis and Brønsted acid sites could be one of the reasons for the selectivity of ethene or diethyl ether (Fig. 7b), because intramolecular and intermolecular dehydration may go through different catalytic sorption processes. However, from our results, the participation of surface OH groups or electron-deficient aluminum atoms in the synthesis of diethyl ether or ethene cannot be ruled out because products formations do not seem to depend on the relative amount of both acid sites.

The temperature evolution of the dehydration reaction for the mesoporous sample Al-1 and for the macroporous one Al-4 are compared in Fig. 7a while 7b shows the product selectivity as a function of conversion. The results show that sample Al-4 was the most active in the whole range of the evaluated temperature, evidencing that the introduction of macropores in the catalyst structure enhanced the ethanol conversion, probably due to transport effects.

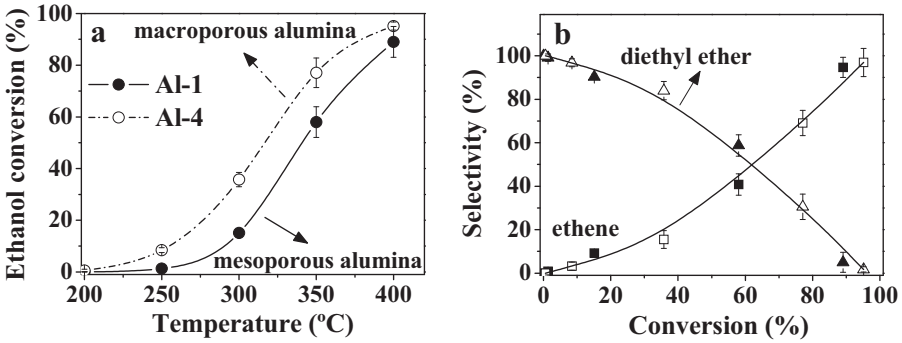

Fig. 7. Catalytic results of ethanol dehydration on mesoporous Al-1 (closed symbols) and macroporous Al-4 (opened symbols) aluminas samples at different temperatures: (a) ethanol conversion and (b) product selectivity as a function of the conversion.

4. Conclusions

Alumina catalysts with varying porosity were prepared by the combination of the sol–gel method and templating with micelle and emulsion. For the obtained morphologies the catalytic activity in ethanol dehydration went through a minimum as a function of samples porosity. This behavior can be explained by the combination of surface acidity and porosity. The results clearly show that macroporous alumina with well designed pore structure allows for a rapid diffusion and consequently improve the reaction kinetics. However, especial attention must be given to the synthesis procedure, because the addition of decahydronaftalene as "oil phase" negatively interfered on the concentration of superficial hydroxyl and consequently in the alumina acidity. This work highlights that both porosity and acidity must be considered in the evaluation of the overall activity of porous catalysts prepared by similar procedures.

Acknowledgments

We are deeply grateful to CNPq and FAPESP for the financial support offered.

References

[1] K. Tanabe, W.F. Holderich, Appl. Catal. A: Gen. 181 (1999) 399–434.
[2] G. Ertl, H. Knözinger, J. Weitkamp, Preparation of Solid Catalysts, Wiley-VCH, 1999.
[3] R. Takahashi, S. Sato, T. Sodesawa, K. Arai, M. Yabuki, J. Catal. 229 (2005) 24–29.
[4] L. Martins, M.A.A. Rosa, S.H. Pulcinelli, C.V. Santilli, Micropor. Mesopor. Mater. 132 (2010) 268–275.
[5] M.A.A. Rosa, E.P. Santos, C.V. Santilli, S.H. Pulcinelli, J. Non-Cryst. Solids 354 (2008) 4786.
[6] T. Numaguchi, Catal. Surv. Jpn. 5 (2001) 59–63.
[7] C. Marquez-Alvarez, N. Zilkova, J. Perez-Pariente, J. Cejka, Catal. Rev.-Sci. Eng. 50 (2008) 222.
[8] D.P. Fabiano, B. Hamad, D. Cardoso, N. Essayem, J. Catal. 19 (2010) 190–196.
[9] E.W. Washburn, Proc. Natl. Acad. Sci. U.S.A. 7 (1921) 115.
[10] R. Rinaldi, F.Y. Fujiwara, U. Schuchardt, Appl. Catal. A: Gen. 315 (2006) 44–51.
[11] J.J. Fitzgerald, G. Piedra, S.F. Dec, M. Seger, G.E. Maciel, J. Am. Chem. Soc. 119 (1997) 7832–7842.
[12] S. Carre, B. Tapin, Appl. Catal. A: Gen. 372 (2010) 26–33.
[13] J.I. Di Cosimo, V.K. Diez, M. Xu, E. Iglesia, C.R. Apesteguia, J. Catal. 178 (1998) 499–510.
[14] R. Takahashi, S. Sato, S. Tomiyama, T. Ohashi, N. Nakamura, Micropor. Mesopor. Mater. 98 (2007) 107–114.
[15] S.-W. Bian, Y.-L. Zhang, H.-L. Li, Y. Yu, Y.-L. Song, W.-G. Song, Micropor. Mesopor. Mater. 131 (2010) 289–293.
[16] J.R. Jain, C.N. Pillai, J. Catal. 9 (1967) 322–330.